



Published in final edited form as:

Langmuir. 2013 December 10; 29(49): 15336–15349. doi:10.1021/la403370p.

Dynamic Measurements of Membrane Insertion Potential of Synthetic Cell Penetrating Peptides

Nabil A. Alhakamy¹, Anubhav Kaviratna², Cory J. Berklund^{1,2}, and Prajnaparamita Dhar^{2,*}¹Department of Pharmaceutical Chemistry, University of Kansas, Lawrence, KS, USA 66047²Department of Chemical & Petroleum Engineering, University of Kansas, Lawrence, KS, USA 66047

Abstract

Cell penetrating peptides (CPPs) have been established as excellent candidates for mediating drug delivery into cells. When designing synthetic CPPs for drug delivery applications, it is important to understand their ability to penetrate the cell membrane. In this paper, anionic or zwitterionic phospholipid monolayers at the air-water interface are used as model cell membranes to monitor the membrane insertion potential of synthetic CPPs. The insertion potential of CPPs having different cationic and hydrophobic amino acids were recorded using a Langmuir monolayer approach that records peptide adsorption to model membranes. Fluorescence microscopy was used to visualize alterations in phospholipid packing due to peptide insertion. All CPPs had the highest penetration potential in the presence of anionic phospholipids. In addition, two of three amphiphilic CPPs inserted into zwitterionic phospholipids, but none of the hydrophilic CPPs did. All the CPPs studied induced disruptions in phospholipid packing and domain morphology, which were most pronounced for amphiphilic CPPs. Overall, small changes to amino acids and peptide sequences resulted in dramatically different insertion potentials and membrane reorganization. Designers of synthetic CPPs for efficient intracellular drug delivery should consider small nuances in CPP electrostatic and hydrophobic properties.

Keywords

Cell penetrating peptides; Langmuir; Surface pressure; Amphiphilic; Hydrophilic; Phospholipid monolayers; POPG; POPC; DPPC

1. Introduction

Recent research has seen an accelerated development of vectors that aid in the delivery and/or cellular uptake of therapeutic macromolecules (e.g. small peptides, proteins, and nucleic acids)^{1, 2, 3, 4}. Cell penetrating peptides (CPPs) are one of the most efficient and promising non-viral vectors that allow transport of large, hydrophilic biomacromolecules through the seemingly impenetrable plasma membrane without cellular rupture^{5, 6, 7, 8}. CPPs normally constitute between 5–30 amino acid sequences, are cationic, can display low toxicity, and are uniquely capable of transporting even negatively charged DNA or siRNA through the cell membrane and nuclear membrane. They can generally be divided into three categories, depending on their origin: protein-derived CPPs such as HIV-TAT and penetratin, chimeric peptides like transportan and MPG and synthetic peptides such as polylysine, polyarginine

*Corresponding Author: Address: 4132 Learned Hall 1530 W 15th St Lawrence, KS 66045 Telephone: (785) 864-4969; Fax: (785) 864-4967; prajnadhar@ku.edu..

or amphipathic versions of these peptides^{8,9}. While it is now well accepted that the mechanism of penetration is not receptor-mediated and is energy-independent^{4, 10, 11}, the exact mechanisms of cellular uptake of these CPPs remains a significant unanswered piece of the puzzle^{8, 12}. The absence of signs of internalization by known uptake mechanisms has led to the proposal that direct interactions with the phospholipid of plasma membrane is an important first step during the early stages of the internalization process¹³.

Since most CPPs generally have a high content of cationic amino acids such as lysine and arginine, experimental observations have predominantly stressed the role of electrostatic interaction of cationic CPPs with negatively charged phospholipid headgroups or negatively charged cell membrane proteoglycans as the primary triggers for internalization^{4, 14, 15}. A few studies have also suggested that hydrophobic interactions, or membrane curvature may influence the early stages of internalization¹⁶. The nature of the CPPs (e.g. molecular weight, chemical structure of the residues, charge, and hydrophilicity) influence the internalization mechanisms^{8, 14}. For example, strong experimental evidence suggests that arginine residues play an important role in membrane penetration. Consequently, studies to determine the factors that improve cellular penetration of natural and synthetic arginine-rich CPPs is an important research effort¹⁷.

The TAT peptide (derived from the transcriptional activator of the HIV-1 virus) is one of the most extensively studied arginine-rich CPPs, and has been shown to interact strongly with model membranes^{18, 19}. As a result, synthetic arginine-rich polypeptides offer great potential for application in efficient drug delivery, particularly by altering the patterning of the amino acid sequence. For example, polyarginine peptides (e.g. R9) with high potency^{6, 20} have been advanced by the insertion of hydrophobic residues^{1, 21, 22}. Rydberg et al. demonstrated that the penetration efficiency increases with increased tryptophan content (a hydrophobic amino acid); additionally, the CPP activity is more efficient if the tryptophan residues are positioned as a block in the center of the CPP sequences than if they are placed as a block at the N-terminus¹. Higher polyarginine molecular weight can promote more efficient penetration^{23, 24}, but optimal lengths of polyarginine peptides with 7 to 9 residues^{25, 26} have shown high penetration activity as well^{1, 23, 27}.

Identification of the mode of penetration of CPPs is essential for the design of future CPPs and forms the main motivation of this study. Phospholipid monolayers are extensively used as a model for one leaflet of the cell membrane^{28, 29, 30, 31}, the charge density and packing of which can be simply adjusted by altering the phospholipid composition and/or surface pressure²⁸. Here, the mechanisms of insertion of eight different synthetic CPPs were compared using three different phospholipid monolayers. 1-palmitoyl-2-oleoyl-sn-glycero-3-phosphatidylglycerol (POPG) (unsaturated phospholipids), 1-palmitoyl-2-oleoyl-sn-glycero-3-phosphocholine (POPC) (unsaturated phospholipids), and 1, 2-dihexadecanoyl-sn-glycero-3-phosphocholine (DPPC) monolayers (saturated phospholipids) (Table 1) at the air-water interface were chosen as the phospholipids of interest. POPG was used as a model anionic monolayer, POPC and DPPC were used as model zwitterionic monolayers, and a 1:1 mixture of DPPC:POPG was used to study the effect of charge density on CPP insertion. By keeping the phospholipid monolayer area constant, changes in S.P are recorded upon addition of CPPs to the subphase^{32, 33, 34, 35}. Even if eukaryotic plasma membranes are mostly composed of zwitterionic phospholipids in their external layer, a very small proportion of anionic phospholipids is also present. It must also be noted that the external leaflet of the plasma membrane contains a high amount of negative charges due to the presence of glycosaminoglycans such as heparan sulfate at the cell surface. It is therefore hypothesized that negatively charged lipids, although small in number, and glycosaminoglycans play a significant role in the mechanism of internalization of the positively charged CPPs, by facilitating electrostatic interactions with the cell

membrane^{6, 36, 37, 38}. Therefore, in accordance with previous studies in this area, POPG was chosen as a representative negatively charged phospholipid for our studies.

Alterations in the membrane packing as well as the peptides' penetration activity at the air/phospholipid monolayer interface was studied for five hydrophilic CPPs (dTAT, R9, L9, H9, and RH9) and three amphiphilic CPPs (RA9, RL9, and RW9) (Table 2). Most of these CPPs share a common high density of arginine residues (6 arginine residues) except for K9 and H9. Our choice of peptides is influenced by previous research in this area. R8 and R9 are the most extensively studied arginine-rich peptides, and are inspired by the highly basic minimal transduction domain of the HIV-1 TAT protein, typically consisting of 9 amino acids (RKKRRQRRR)³⁹. Based on prior reports^{1, 37, 40}, four of the arginine rich CPPs (RH9, RA9, RL9, and RW9) have replaced the arginine residues at positions 3, 4 and 7 with histidine, alanine, leucine, or tryptophan in order to study the effect of amino acid patterning on the penetration activity.

2. Materials and methods

2.1. Materials

dTAT (RKKRRQRRRHRRKKR; Mw = 2201.7 Da) peptide, H9 (HHHHHHHHH; Mw = 1251.38 Da) peptide, K9 (KKKKKKKKK; Mw = 1170.65 Da) peptide, R9 (RRRRRRRRR; Mw = 1422.74 Da) peptide, RH9 (RRHRRRHRR; Mw = 1365.62 Da) peptide, RA9 (RRAARRARR; Mw = 1167.41 Da) peptide, RL9 (RLLRRLRR; Mw = 1293.68 Da) peptide, and RW9 (RRWRRRWRR; Mw = 1512.83 Da) peptide were purchased from Biomatik Corporation (Cambridge, Ontario, Canada) (Purity > 95%). 1-palmitoyl-2-oleoyl-sn-glycero-3-phospho-(1'-rac-glycerol) (sodium salt) (POPG), 1-hexadecanoyl-2-(9Z-octadecenoyl)-sn-glycero-3 phosphocholine (sodium salt) (POPC), and 1,2-dipalmitoyl-sn-glycero-3-phosphocholine (DPPC) were purchased from Avanti Polar Lipids, Alabaster, AL, as organic mixtures in chloroform at a final concentration of 5 mg/ml. Texas Red® 1,2-dihexadecanoyl-sn-glycero-3-phosphoethanolamine, triethylammonium salt, (TXR-DHPE) lipid dye was purchased in the dried form from Life Technologies (Invitrogen Corp., Carlsbad, CA, USA). All organic solvents used for this work was purchased from Fisher Scientific. Dulbecco's phosphate-buffered saline (PBS) (pH 7.4) was purchased from Fisher Scientific Inc. in powder form and made into solution using a Millipore Gradient System (Billerica, MA). Petri dishes (Falcon 1008, Becton-Dickinson Labware, Franklin Lakes, NJ) were purchased from Fisher Scientific. All samples and lipid mixtures were stored at -20 °C when not in use.

2.2. Methods

2.2.1. Langmuir trough experiments—The insertion potential of the different synthetic CPPs was measured using model phospholipid monolayers containing different amounts of a negatively charged phospholipid (POPG, POPC, DPPC, POPG/DPPC (1:1)) at the air-PBS buffer interface. Surface pressure changes were recorded by a Wilhelmy plate sensor, which is part of the KSV-NIMA Langmuir trough purchased from Biolin Scientific, while petri dishes (volume 4 ml, 35 × 10) were used as “mini-troughs” for the experiments that did not involve fluorescence imaging. Penetration of the CPPs into preformed monoalayers was recorded in the presence of the phospholipid monolayers. A wet calibrated filter paper flag was dipped into this buffer solution and used as a probe to monitor changes in the surface pressure due to adsorption of surface active material. The phospholipid monolayers were spread from chloroformic solutions, on PBS subphase, pH 7.4, using a Hamilton microsyringe (Hamilton Co., Reno, NV). The spreading phospholipid solvents were allowed to evaporate for 20 min prior to compression and adding the CPPs. The CPPs aqueous solutions were injected underneath the surface of phospholipid monolayers, and the changes

in surface pressure with respect to time were measured immediately. The final concentration of the CPPs in the subphase was maintained at 10 μM (using dTAT, RW9, and RL9 this concentration was found to be beyond a so called “saturation concentration”). The peptide-to-lipid (P/L) molar ratio at an initial surface pressure of 20 and 30 mN/m is ≈ 0.5 (at peptide concentration 1 μM)⁵. Precaution was taken to ensure that the injection did not disrupt the phospholipid monolayer. Adsorption to a bare air-buffer interface was recorded for all the CPPs studied here to ensure that the changes in the surface pressure of the monolayers were due to interaction of the CPPs. Each experiment was run for 30 min at 22 ± 2 °C.

2.2.2. Fluorescence Microscopy—Fluorescence microscopy was used concurrently with penetration experiments to monitor the morphology of the phospholipid monolayers on insertion of CPPs. These measurements were performed using a Teflon trough (volume 40 ml, area 174×50 mm) adapted for microscopy (Biolin Scientific). The Langmuir trough was mounted on a Leica DM fluorescence microscope with a custom designed stage equipped with a $10\times$ or $40\times$ long working distance objective designed for fluorescent light. A dichoric mirror/barrier filter assembly directed the excitation light onto the monolayer films at a normal angle of incidence and filtered the emitted light. An 89 North PhotoFluor II 200 W Metal Halide lamp was used for excitation of the probe. Alterations in the surface morphology of the phospholipid monolayers due to the CPPs were visualized with a fast camera (Andor Luca S). Short image sequences (5 frames) were recorded for a period of 30 minutes and stored for further analysis using the Andor capture software. The image processing and analysis were performed offline by using the software, ImageJ 1.47 (NIH) for windows.

It must be noted that unsaturated phospholipid films such as POPG and POPC do not display any lipid domains, when viewed using the fluorescence microscopy technique. Therefore, a 1:1 mixture of DPPC:POPG was used for all imaging experiments. To initiate each experiment, the trough was cleaned with methanol, ethanol, isopropanol and chloroform and thoroughly rinsed with Mili-Q water prior to each experiment. A mixed DPPC/POPG monolayer with 1% TXR-DHPE dye was formed by spreading an organic mixture of this lipid composition dropwise onto 38 ml of a PBS buffer subphase (at pH=7.4), using a Hamilton airtight glass syringe. The solvent was allowed to evaporate completely, by waiting 30 minutes before starting a measurement. Changes in surface pressures with time were recorded by a Wilhelmy plate sensor. The concentration of the CPPs used was such that the final concentration in the subphase is 10 μM . Images from at least two different monolayers for each sample were taken, and the lens frequently translocated to different areas of the trough to ensure uniformity and reproducibility of the data.

2.2.3. Statistical analysis—Data were analyzed by using GraphPad software. Statistical evaluation between the means of the data was performed using an unpaired *t*-test. One-way ANOVA, Tukey post test was used to analyze the differences when more than two data sets were compared. Each monolayer penetration experiment was repeated at least three times ($n = 3$).

3. Results and discussion

A Langmuir monolayer approach coupled with fluorescence microscopy was used to determine the differences in ability of the synthetic CPPs to penetrate into cell membranes. Phospholipid monolayers with varying composition and headgroup charges representing one leaflet of a cell membrane were used as model membranes. Penetration to a phospholipid membrane is typically recorded by one of two methods, a constant area method or constant surface pressure method. In constant area method used here, the surface pressure of the

phospholipid monolayer is fixed at a particular surface pressure (here 20 mN/m and 30 mN/m). Membrane insertion of injected peptide is accompanied by an increase in the surface pressure, since the area of the trough surface is kept constant. Using a fluorescence microscope, we also directly visualize the changes in packing of lipid domains due to peptide insertion. Insertion of the peptides is expected to alter the monolayer packing. Since contrast in the images is due to the selective segregation of the lipid dye into more fluid regions, disruptions in monolayers manifest themselves as an increase in bright regions when compared with a well-packed film.

3.1. Penetration of CPPs into POPG phospholipid monolayers

In order to establish a correlation between the chemical structure of the CPPs and their penetration activity, we recorded their affinity to insert into phospholipid monolayers with different compositions of an anionic phospholipid. We used POPS as the phospholipid of choice, since the penetration of TAT to this phospholipid monolayer has previously been reported. It was reported that TAT demonstrated an inability to penetrate the monolayer at bilayer equivalent surface pressures⁵. Therefore, as a first step increasing amounts of CPPs (dTAT, R9, and RW9) were injected into PBS subphase and alterations in the surface pressure recorded.

Figure 1, shows changes in surface pressure as a function of peptide concentration (1, 5, 10 and 20 μ M) for dTAT (Figure 1A), R9 (Figure 1B), and RW9 (Figure 1C), keeping the initial pressure of POPS to be 20 mN/m. The saturation surface pressure attained in each case as a function of concentration of the CPPs is summarized in Figure 1D. Our results illustrate that the surface pressure increased in each case, reaching a saturation plateau after about 10 to 30 min after injection for all penetration experiments which indicates quick migration of the CPPs to the phospholipid monolayers. However, the time taken to reach a saturation value also depended on the bulk concentration of protein. Further, Figure 1D indicates that a statistically significant difference was observed in the penetration ability of the three peptides. RW9 (maximum change in surface pressure of 11.26 mN/m,) interacted more strongly with the monolayer, when compared with dTAT (the gold standard) and R9 (an arginine rich sequence expected to have high potency in cell penetration). We believe that this increased penetration in case of RW9 may be due to the hydrophobicity or the aromatic ring of tryptophan amino acids, which also increased the amphiphilicity of the peptide. Further, our data show a saturation in the total change in surface pressure for all three cases, beyond a concentration of 10 μ M, which appears to be a “critical concentration”. Therefore, this concentration was chosen for all other studies described in this paper⁵.

In order to better understand the impact of phospholipid packing on peptide insertion, the kinetics of surface pressure changes as a function of time, following dTAT injection into the subphase were studied at different initial surface pressures (0, 15, 20, 30, and 40 mN/m) as shown in Figure 2A. The total change in surface pressure in the presence of dTAT resulted in increased maximum surface pressure values (Figure 2B) at the initial surface pressures (15, 20, and 30 mN/m) due to the fact that packing of the phospholipids is not so dense (low phospholipid densities) to facilitate dTAT peptides to attach and penetrate. On the other hand, penetration decreased when the phospholipid packing density increased (the initial surface pressure 40 mN/m). At a high initial surface pressure (40 mN/m), there is a limited incorporation of the CPP into the phospholipid monolayer, and the process is much slower. From the figures, we conclude that the maximum surface pressure value is at the initial surface pressure 20 mN/m. Therefore, in addition to the bilayer equivalent pressure of 30 mN/m, we also report the insertion of our peptides at an initial surface pressure of 20 mN/m.

Figure 3 illustrates the changes in the surface pressure of the POPG monolayers as a function of time, following interactions with eight CPPs (10 μ M) at initial surface pressures of 20 mN/m (Figure 3A) and 30 mN/m (Figure 3B). It is clear from the figures that the kinetics of insertion of RW9 and RL9 are dramatically faster than the other CPPs. Figures 3C and 3D present the maximum change in surface pressure for each of the eight peptides, when injected below a POPG monolayer held at an initial surface pressure of 20 mN/m (Figure 3C) or 30 mN/m (Figure 3D). From these figures, it is clear that for both surface pressures, the change in surface pressure with time is significantly higher for RW9 and RL9 compared to other CPPs ($p > 0.0001$). It must also be noted that the hydrophilic CPPs (dTAT, H9, K9, R9, and RH9) and RA9 do exhibit moderate surface activities (as indicated by an increase in the total surface pressure).

Phospholipid monolayers are used as model systems to study insertion of biomolecules and/or other particles into biological membranes. Such studies have been exhaustively used to study interaction of antimicrobial peptides with membranes^{30, 41}. Since CPPs share some commonalities with antimicrobial peptides, in this study, we have used these model membranes to gain insight into the biophysical mechanisms of interaction in case of synthetic CPPs. In general, it is now accepted that particles that interact only with the head groups of phospholipid monolayers typically induce slight changes in surface pressure. On the other hand, insertion into the hydrophobic “tail” region (the fatty acyl core) of the phospholipid monolayer can cause a significant increase in surface pressure⁴¹. Although numerous studies were interested in the “arginine magic”, i.e. the ability of arginine rich peptide sequences to penetrate the cell membrane, only a limited number of studies dealt with model systems (e.g. dTAT and R9) to explain the binding mechanism of polyarginine peptides to phospholipid membranes¹⁷. It has been shown that physical characteristics (e.g. the hydrophobicity/hydrophilicity and the surface charge) of CPPs can influence their binding with phospholipid monolayers³². However, to the best of our knowledge, the influence of introducing other amino acids into an arginine sequence has not been extensively studied in model phospholipid systems, such as those described here¹. Our results suggest that the introduction of tryptophan and leucine residues into polyarginine 9 improve the penetration activity significantly.

Additionally, numerous studies have mentioned the importance of peptide structural conformational changes upon phospholipid interactions to facilitate membrane translocation^{42, 43, 44}. It was found that the different penetration properties of the cationic CPPs and amphiphilic CPPs may arise from the insertion mechanism into phospholipid monolayers³⁷. Walrant et al. indicated that while RW9 and RL9 have an affinity for anionic phospholipids, the affinity is just a little higher for RW9 than RL9. The interactions are mostly ruled by hydrophobic assistances in both CPPs^{6, 37}. Additionally, they found that a flip of the CPP occurs where the arginine residues aid as a hinge letting the hydrophobic amino acids insert deeper in the plasma membrane³⁷. Although alanine is a hydrophobic amino acid, RA9 demonstrates only a moderate surface activity when compared to RW9 and RL9. This behavior is possibly be due to the chemical structure of the hydrophobic residues; alanine has a very small side chain when compared with the more bulky tryptophan. Before studying the incorporation of the CPPs with the phospholipid monolayers, we examined the behavior of the eight CPPs at a bare air/water interface by using the Langmuir technique described above in the absence of the phospholipids (Supplementary Figure 1 in the Supporting Information). All eight CPPs showed no or little surface activity for the 30 min duration, which is in agreement with the nature of the five hydrophilic CPPs (dTAT, H9, K9, and RH9) and weak amphiphilic characters of the three CPPs (RA9, RL9, and RW). These results indicate that the change in surface pressure recorded in Figure 3 is clearly due to interactions with the anionic phospholipid films.

3.2. Penetration of the CPPs in DPPC and POPC phospholipid monolayers

In order to test the effect of electrostatic interactions vs. hydrophobic interactions on the insertion potential of these synthetic peptides into model membranes, we compare the insertion potential of the eight CPPs into zwitterionic monolayers (POPC (unsaturated) and DPPC (saturated)) compared with the POPG monolayer. Figure 4A shows the change in surface pressure as a function of time, for the POPC film initially held at a surface pressure of 20 mN/m. As seen in the figure, low penetration activity was observed for the synthetic peptides, except for RW9 and RL9. In fact, the penetration activity of RW9 and RL9 is found to be significantly higher than the other CPPs. Figure 4B shows the change in surface pressure vs. time for an initial surface pressure of 30 mN/m. The maximum surface pressures reached in each case is summarized in bar graphs in Figure 4C and 4D. As seen, both RW9 and RL9 have significant surface activity compared to other CPPs ($p > 0.0001$) as shown by the maximum values of 5.9 and 4.3 mN/m respectively (at the initial surface pressure of 20 mN/m) and 3.7 and 1.9 mN/m respectively (at the initial surface pressure of 30 mN/m). In contrast, even though RA9 is an amphiphilic peptides, it does not display significant insertion into the POPC films. Figure 5 presents a summary of the comparison of the maximum surface pressure values that were recorded at a concentration of 10 μM (the initial surface pressures 20 mN/m (Figure A) and 30 mN/m (Figure B)) for the eight CPPs, for an anionic phospholipid film (POPG) and a zwitterionic phospholipid film (POPC). This graph clearly indicates that anionic phospholipid head groups play an important role for interactions with the eight CPPs. However, for two of the three arginine-rich peptides modified by hydrophobic residues, the membrane penetration potential is significantly enhanced.

Figure 6A shows the change in surface pressure as a function of time, for the DPPC (more tightly packed monolayer) film initially held at a surface pressure of 20 mN/m. As seen in the figure, no penetration activity was observed for the synthetic peptides, except for RW9 and RL9. In fact, the penetration activity of RW9 and RL9 is found to be significantly higher than the other CPPs. Figure 6B shows the change in surface pressure vs. time for an initial surface pressure of 30 mN/m. For clarity, we only show the change in surface pressure for RW9 and RL9. The maximum surface pressures reached in each case is summarized in bar graphs in Figure 6C and 6D. As seen, both RW9 and RL9 have significant surface activity compared to other CPPs ($p > 0.0001$) as showed by the maximum values of 4.0 and 1.7 mN/m respectively (at the initial surface pressure of 20 mN/m) and 4.5 and 0.6 mN/m respectively (at the initial surface pressure of 30 mN/m). The smaller penetration activity for zwitterionic DPPC monolayers (saturated phospholipids) in some CPPs when compared to anionic POPG and POPC (both unsaturated phospholipids) monolayers indicate weak interactions between the CPPs and DPPC. The reduced insertion of all but RW9 into the DPPC phospholipid monolayer may also be the result of a well-packed monolayer preventing CPPs insertion.

Figure 6 also shows that the penetration activity of RW9 is significantly higher than RL9 or RA9 in both initial surface pressures, even though all three of these arginine-rich peptides were modified by hydrophobic moieties. It was found that the addition of one tryptophan residue to a polyarginine 7 peptide (R7) increased its penetration efficiency⁴⁵. Clearly, tryptophan residue has a key role in cell penetration, possibly due to the bulky side chains^{1, 37, 46, 47}. In summary, our results show that in addition to electrostatic effects, hydrophobic interactions as well as the chemical nature of the amino acids do influence the differences in membrane penetration potential of the CPPs.

3.3. Penetration of the CPPs in mixed (POPG:DPPC) phospholipid monolayers

The mixing properties of a mixed monolayer of DPPC and POPG was used as a model to understand the role of different composition of the anionic phospholipid headgroup on peptide insertion in order to simultaneously image the insertion and possible alterations in monolayer packing. We have chosen this mixture to be consistent with the fluorescent microscopy experiments (section 3.4.). The mixture of saturated PC (DPPC) phospholipids and fluid unsaturated PG (POPG) phospholipids have been used so that lipid domains can be observed.

Figure 7 shows change in surface pressure of a mixed phospholipid film as a function of time, for the eight CPPs (10 μ M) at the initial surface pressure 20 (Figure 7A) and 30 mN/m (Figure 7B). Our results indicated that reducing the surface charge density of the phospholipid monolayers by using mixed phospholipids (POPG/DPPC) caused a decrease in the surface pressure. Figure 7C and 7D summarize the maximum change in surface pressure for the eight CPPs. Our results show that the hydrophilic CPPs (dTAT, H9, K9, R9, and RH9) and RA9 have moderate surface activity when the maximum surface pressure values are between 1.5 and 3.0 mN/m (the initial surface pressure 20 mN/m) and between 1.2 and 2.6 mN/m (the initial surface pressure 30 mN/m). Conversely, RW9 and RL9 have large surface pressure increases as shown by the maximum values of 8.0 and 9.4 mN/m, respectively, (the initial surface pressure 20 mN/m) and 5.6 and 4.9 mN/m respectively (the initial surface pressure 30 mN/m). Figure 8 presents the summary of the maximum surface pressure values that were recorded at a concentration of 10 μ M (the initial surface pressures 20 and 30 mN/m) for the eight CPPs, for all four phospholipid films (POPG, POPC, DPPC and, POPG:DPPC). This summary clearly indicates that while anionic phospholipid headgroups play the most important role for interactions with the hydrophilic CPPs (dTAT, H9, K9, R9, and RH9), the insertion of the arginine peptides is also significantly influenced by the presence of tryptophan residues.

To further our understanding of the role of the 3D peptide structure on the insertion potential of the CPPs, we used circular dichroism spectroscopy (CD) to determine the helicity of the eight CPPs in PBS solution (Supplementary Figure 2 in the Supporting Information). Our data confirmed that the free CPPs had random coil conformations, suggesting that the initial steps in peptide insertion are not influenced by the 3-D structure. However, NMR, CD and molecular dynamics simulation studies by other groups have shown that insertion into the lipid bilayers can induce different degrees of structural re-orientation depending on the amino acid sequence^{6, 48, 40, 49}. This may also explain the differences in a peptide's ability to translocate through the membrane. Therefore, we conclude that while the 3D structure in solution does not seem to influence the surface activity of the 8 CPPs, the penetration and translocation through cell membranes may be influenced by a lipid bilayer induced alteration in the protein structure. This suggests that while the surface pressure changes in a Langmuir trough may be a good screening test to determine the penetration potential of synthetic peptides into cell membranes, the ultimate translocation potential of the peptide may be dictated by their 3-D structure upon membrane penetration.

It is expected that analysis of the kinetics and thermodynamics of the 8 CPPs will provide a more complete understanding of the nature of the CPP partitioning into the phospholipid monolayers. Using Langmuir models of protein insertion into phospholipid monolayers^{50, 51, 52, 53, 54, 55, 56}, we can calculate the kinetics of protein partitioning into different monolayer systems. Such analysis will form the topic for a future manuscript currently under preparation.

3.4. Fluorescence microscopy

Using fluorescence imaging of the monolayer surface, it is possible to gain insight into the structure of the phospholipid monolayers. Fluorescence microscopy helps us to understand alterations in organization of phospholipid monolayers after injection of the CPPs in the subphase. Furthermore, it is an appropriate effective technique to study the structural phase separation and disruption induced by CPP interactions with phospholipid monolayers^{30, 57}. Figure 9A demonstrates the morphology of the POPG/DPPC (1:1) phospholipid monolayer domains (at the surface pressure 30 mN/m) before injection the CPPs. It shows characteristic stripe patterns with dark regions (the bright regions in the dark domains looked like veins in a leaf). Contrast in these images is due to selective segregation of the lipid dye molecules into the liquid expanded regions, while the closely packed liquid condensed domains exclude the bulky dye molecules. The domains were magnified as compression proceeded, and the view field becomes almost dark⁵⁸ at the bilayer equivalent pressures studied here. The images were obtained at 1, 5, 10, 20, and 30 min, respectively after injection of the CPPs into the subphase.

Remarkably, the domain morphology altered significantly depending on the nature of the CPP. The images display that CPPs induce different morphologies even at the first minute after injection. In the case of dTAT, H9, K9, R9, RH9, and RA9 (Figure 9B, C, D, E, F, and G, respectively), the overall change in the domain morphology is limited (a very slight increase in the gray regions) for the first 10 minutes (after the CPP injected) except for RW9. In case of RW9 (Figure 9I), within 10 minutes of CPP injection, the dark domains completely disappeared (no domains could be observed) nearly after five min of the injection. Interestingly, after 20 minutes the morphologies of the domains were vividly different for all CPPs. In the case of RL9 (Figure 9H), blurred gray patches began to appear, while all other CPPs showed an increase in the brightness and width of the stripe pattern. At 30 minutes all of the peptides (except H9) showed either blurred gray patches, or more disrupted monolayers like RL9 and RW9. Our results also show that H9 shows the minimum perturbation of the phospholipid packing among all the CPPs studied, even after 30 minutes (darker domains are still visible). Moreover, the arginine-rich peptides all induce significantly higher changes in the phospholipid packing compared to dTAT. Peptide RW9 demonstrates the maximum disruption of monolayer packing, followed by RL9 and RA9. R9 and RH9 seem to induce very similar membrane perturbation.

In general, our results reinforce the role of not only electrostatics and hydrophobic interactions, but also the chemical nature of amino acids on the membrane penetration potential of CPPs. While all CPPs show the maximum membrane penetration in the presence of anionic headgroups, amphiphilic CPPs with tryptophan residues show a significant membrane insertion potential for all model lipid monolayers. Moreover, we present direct evidence of destabilization of phospholipid packing induced by amphiphilic arginine-rich CPPs, which is also most pronounced by the presence of tryptophan residues.

4. Conclusion

Understanding the interactions of synthetic CPPs with phospholipid membranes is an important step when designing future synthetic CPPs capable of intracellular drug delivery. In this study, phospholipid monolayers with different composition of anionic headgroups (POPG, POPE, DPPC, or POPG/DPPC) have been used to study the penetration, and/or interaction with eight synthetic peptides including hydrophilic CPPs (dTAT, H9, K9, R9, and RH9) and the amphiphilic CPPs (RA9, RL9, and RW9). Insertion of the CPPs into the phospholipid monolayers were followed using Langmuir monolayer techniques and fluorescence microscopy. As expected, the incorporation of the cationic CPPs into the

anionic phospholipids (POPG) was much higher when compared with the zwitterionic phospholipids (POPC and DPPC).

In addition to electrostatic interactions, hydrophobic interactions as well as the chemical nature of the amino acid residues influenced the membrane insertion potential. The presence of tryptophan residues induced maximum perturbation of the phospholipid packing. All CPPs interacted with anionic phospholipids, but the interactions of RW9 and RL9 with membrane monolayers was significantly different when compared with the other peptides. RW9 and RL9 strongly penetrated the model cell membranes and also induced the maximum alterations in phospholipid packing. The five hydrophilic CPPs (dTAT, R9, L9, H9, and RH9) and RA9 peptides also showed penetration into the model membranes, but did not appear to cause significant membrane disruption. The different mechanisms of the eight CPPs compel additional investigations using these CPPs for delivery of macromolecules in cellular systems. Further elucidating performance in light of these mechanistic findings will aid the design of the next generation of CPPs.

Supplementary Material

Refer to Web version on PubMed Central for supplementary material.

Acknowledgments

We would like to acknowledge financial support from the following sources: Higuchi Biosciences Center, and the NIH (P20 GM103638).

References

- Rydberg HA, Matson M, Åmand HL, Esbjörner EK, Nordén B. Effects of tryptophan content and backbone spacing on the uptake efficiency of cell-penetrating peptides. *Biochemistry*. 2012; 51(27): 5531–5539. [PubMed: 22712882]
- Ziello JE, Huang Y, Jovin IS. Cellular endocytosis and gene delivery. *Molecular Medicine*. 2010; 16(5–6):222. [PubMed: 20454523]
- Guo J, Bourre L, Soden DM, O'Sullivan GC, O'Driscoll C. Can non-viral technologies knockdown the barriers to siRNA delivery and achieve the next generation of cancer therapeutics? *Biotechnology advances*. 2011; 29(4):402–417. [PubMed: 21435387]
- Deshayes S, Morris MC, Divita G, Heitz F. Interactions of amphipathic CPPs with model membranes. *Biochimica et Biophysica Acta (BBA)-Biomembranes*. 2006; 1758(3):328–335.
- Dennison SR, Baker RD, Nicholl ID, Phoenix DA. Interactions of cell penetrating peptide Tat with model membranes: a biophysical study. *Biochemical and biophysical research communications*. 2007; 363(1):178–182. [PubMed: 17854767]
- Walrant A, Correia I, Jiao C-Y, Lequin O, Bent EH, Goasdoué N, Lacombe C, Chassaing G, Sagan S, Alves ID. Different membrane behaviour and cellular uptake of three basic arginine-rich peptides. *Biochimica et Biophysica Acta (BBA)-Biomembranes*. 2011; 1808(1):382–393.
- Fonseca SB, Pereira MP, Kelley SO. Recent advances in the use of cell-penetrating peptides for medical and biological applications. *Advanced drug delivery reviews*. 2009; 61(11):953–964. [PubMed: 19538995]
- Alhakamy NA, Nigatu AS, Berklund CJ, Ramsey JD. Noncovalently associated cell-penetrating peptides for gene delivery applications. *Therapeutic Delivery*. 2013; 4(6):741–757. [PubMed: 23738670]
- Lindgren, M.; Langel, Ü. *Cell-Penetrating Peptides*. Springer: 2011. Classes and prediction of cell-penetrating peptides; p. 3-19.
- Wender PA, Mitchell DJ, Pattabiraman K, Pelkey ET, Steinman L, Rothbard JB. The design, synthesis, and evaluation of molecules that enable or enhance cellular uptake: peptoid molecular transporters. *Proceedings of the National Academy of Sciences*. 2000; 97(24):13003–13008.

11. Derossi D, Calvet S, Trembleau A, Brunissen A, Chassaing G, Prochiantz A. Cell internalization of the third helix of the Antennapedia homeodomain is receptor-independent. *Journal of Biological Chemistry*. 1996; 271(30):18188–18193. [PubMed: 8663410]
12. Hassane FS, Saleh A, Abes R, Gait M, Lebleu B. Cell penetrating peptides: overview and applications to the delivery of oligonucleotides. *Cellular and molecular life sciences*. 2010; 67(5): 715–726. [PubMed: 19898741]
13. Thorén PE, Persson D, Lincoln P, Nordén B. Membrane destabilizing properties of cell-penetrating peptides. *Biophysical chemistry*. 2005; 114(2):169–179. [PubMed: 15829350]
14. Silhol M, Tyagi M, Giacca M, Lebleu B, Vivès E. Different mechanisms for cellular internalization of the HIV-1 Tat-derived cell penetrating peptide and recombinant proteins fused to Tat. *European Journal of Biochemistry*. 2002; 269(2):494–501. [PubMed: 11856307]
15. Magzoub M, Kilk K, Eriksson L, Langel Ü, Gräslund A. Interaction and structure induction of cell-penetrating peptides in the presence of phospholipid vesicles. *Biochimica et Biophysica Acta (BBA)-Biomembranes*. 2001; 1512(1):77–89.
16. Schmidt N, Mishra A, Lai GH, Wong GC. Arginine-rich cell-penetrating peptides. *FEBS Lett*. 2010; 584(9):1806–13. [PubMed: 19925791]
17. Schwieger C, Blume A. Interaction of poly (l-arginine) with negatively charged DPPG membranes: calorimetric and monolayer studies. *Biomacromolecules*. 2009; 10(8):2152–2161. [PubMed: 19603784]
18. Gonçalves E, Kitas E, Seelig J. Binding of oligoarginine to membrane lipids and heparan sulfate: structural and thermodynamic characterization of a cell-penetrating peptide. *Biochemistry*. 2005; 44(7):2692–2702. [PubMed: 15709783]
19. Vivès E, Brodin P, Lebleu B. A truncated HIV-1 Tat protein basic domain rapidly translocates through the plasma membrane and accumulates in the cell nucleus. *Journal of Biological Chemistry*. 1997; 272(25):16010–16017. [PubMed: 9188504]
20. Mitchell D, Steinman L, Kim D, Fathman C, Rothbard J. Polyarginine enters cells more efficiently than other polycationic homopolymers. *The Journal of Peptide Research*. 2000; 56(5):318–325. [PubMed: 11095185]
21. Thorén PE, Persson D, Isakson P, Goksör M, Önfelt A, Nordén B. Uptake of analogs of penetratin, Tat (48–60) and oligoarginine in live cells. *Biochemical and biophysical research communications*. 2003; 307(1):100–107. [PubMed: 12849987]
22. Thorén PE, Persson D, Esbjörner EK, Goksör M, Lincoln P, Nordén B. Membrane binding and translocation of cell-penetrating peptides. *Biochemistry*. 2004; 43(12):3471–3489. [PubMed: 15035618]
23. Rothbard JB, Kreider E, VanDeusen CL, Wright L, Wylie BL, Wender PA. Arginine-rich molecular transporters for drug delivery: role of backbone spacing in cellular uptake. *Journal of medicinal chemistry*. 2002; 45(17):3612–3618. [PubMed: 12166934]
24. Takechi Y, Yoshii H, Tanaka M, Kawakami T, Aimoto S, Saito H. Physicochemical mechanism for the enhanced ability of lipid membrane penetration of polyarginine. *Langmuir*. 2011; 27(11): 7099–7107. [PubMed: 21526829]
25. Futaki S, Goto S, Sugiura Y. Membrane permeability commonly shared among arginine-rich peptides. *Journal of Molecular Recognition*. 2003; 16(5):260–264. [PubMed: 14523938]
26. Futaki S, Nakase I, Tadokoro A, Takeuchi T, Jones A. Arginine-rich peptides and their internalization mechanisms. *Biochemical Society Transactions*. 2007; 35(4):784. [PubMed: 17635148]
27. Wender PA, Galliher WC, Goun EA, Jones LR, Pillow TH. The design of guanidinium-rich transporters and their internalization mechanisms. *Advanced drug delivery reviews*. 2008; 60(4): 452–472. [PubMed: 18164781]
28. Barzyk W, Campagna S, Wiśniewski K, Korchowiec B, Rogalska E. The affinity of two antimicrobial peptides derived from bovine milk proteins for model lipid membranes. *Colloids and Surfaces A: Physicochemical and Engineering Aspects*. 2009; 343(1):104–110.
29. Brockman H. Lipid monolayers: why use half a membrane to characterize protein-membrane interactions? *Current opinion in structural biology*. 1999; 9(4):438–443. [PubMed: 10449364]

30. Volinsky R, Kolusheva S, Berman A, Jelinek R. Investigations of antimicrobial peptides in planar film systems. *Biochimica et Biophysica Acta (BBA)-Biomembranes*. 2006; 1758(9):1393–1407.
31. Brezesinski G, Möhwald H. Langmuir monolayers to study interactions at model membrane surfaces. *Advances in colloid and interface science*. 2003; 100:563–584. [PubMed: 12668338]
32. Peetla C, Stine A, Labhasetwar V. Biophysical interactions with model lipid membranes: applications in drug discovery and drug delivery. *Molecular pharmaceutics*. 2009; 6(5):1264–1276. [PubMed: 19432455]
33. Preetha A, Huilgol N, Banerjee R. Comparison of paclitaxel penetration in normal and cancerous cervical model monolayer membranes. *Colloids and Surfaces B: Biointerfaces*. 2006; 53(2):179–186.
34. Demel R, Geurts van Kessel W, Zwaal R, Roelofsen B, Van Deenen L. Relation between various phospholipase actions on human red cell membranes and the interfacial phospholipid pressure in monolayers. *Biochimica et Biophysica Acta (BBA)-Biomembranes*. 1975; 406(1):97–107.
35. Blume A. A comparative study of the phase transitions of phospholipid bilayers and monolayers. *Biochimica et Biophysica Acta (BBA)-Biomembranes*. 1979; 557(1):32–44.
36. Joanne P, Galanth C, Goasdoué N, Nicolas P, Sagan S, Lavielle S, Chassaing G, El Amri C, Alves ID. Lipid reorganization induced by membrane-active peptides probed using differential scanning calorimetry. *Biochimica et Biophysica Acta (BBA)-Biomembranes*. 2009; 1788(9):1772–1781.
37. Walrant A, Vogel A, Correia I, Lequin O, Olausson BE, Desbat B, Sagan S, Alves ID. Membrane interactions of two arginine-rich peptides with different cell internalization capacities. *Biochimica et Biophysica Acta (BBA)-Biomembranes*. 2012; 1818(7):1755–1763.
38. Jiao C-Y, Delaroche D, Burlina F, Alves ID, Chassaing G, Sagan S. Translocation and endocytosis for cell-penetrating peptide internalization. *Journal of Biological Chemistry*. 2009; 284(49):33957–33965. [PubMed: 19833724]
39. Deshayes S, Morris M, Divita G, Heitz F. Cell-penetrating peptides: tools for intracellular delivery of therapeutics. *Cellular and Molecular Life Sciences CMLS*. 2005; 62(16):1839–1849. [PubMed: 15968462]
40. Witte K, Olausson BE, Walrant A, Alves ID, Vogel A. Structure and dynamics of the two amphipathic arginine-rich peptides RW9 and RL9 in a lipid environment investigated by solid-state NMR and MD simulations. *Biochimica et Biophysica Acta (BBA)-Biomembranes*. 2012
41. Zhang L, Rozek A, Hancock RE. Interaction of cationic antimicrobial peptides with model membranes. *Journal of Biological Chemistry*. 2001; 276(38):35714–35722. [PubMed: 11473117]
42. Sakai N, Futaki S, Matile S. Anion hopping of (and on) functional oligoarginines: from chloroform to cells. *Soft Matter*. 2006; 2(8):636–641.
43. Lins L, Decaffmeyer M, Thomas A, Brasseur R. Relationships between the orientation and the structural properties of peptides and their membrane interactions. *Biochimica et Biophysica Acta (BBA)-Biomembranes*. 2008; 1778(7):1537–1544.
44. Eiríksdóttir E, Konate K, Langel Ü, Divita G, Deshayes S. Secondary structure of cell-penetrating peptides controls membrane interaction and insertion. *Biochimica et Biophysica Acta (BBA)-Biomembranes*. 2010; 1798(6):1119–1128.
45. Maiolo JR, Ferrer M, Ottinger EA. Effects of cargo molecules on the cellular uptake of arginine-rich cell-penetrating peptides. *Biochimica et Biophysica Acta (BBA)-Biomembranes*. 2005; 1712(2):161–172.
46. Yau W-M, Wimley WC, Gawrisch K, White SH. The preference of tryptophan for membrane interfaces. *Biochemistry*. 1998; 37(42):14713–14718. [PubMed: 9778346]
47. Landolt-Marticorena C, Williams KA, Deber CM, Reithmeier RA. Non-random distribution of amino acids in the transmembrane segments of human type I single span membrane proteins. *Journal of molecular biology*. 1993; 229(3):602–608. [PubMed: 8433362]
48. Futaki S, Suzuki T, Ohashi W, Yagami T, Tanaka S, Ueda K, Sugiura Y. Arginine-rich peptides: An abundant source of membrane-permeable peptides having potential as carriers for intracellular protein delivery. *Journal of Biological Chemistry*. 2001; 276(8):5836–5840. [PubMed: 11084031]
49. Bechara C, Pallerla M, Zaltsman Y, Burlina F, Alves ID, Lequin O, Sagan S. Tryptophan within basic peptide sequences triggers glycosaminoglycan-dependent endocytosis. *The FASEB Journal*. 2013; 27(2):738–749.

50. Sánchez-Martín, M. J. s.; Haro, I.; Alsina, MA.; Busquets, MA.; Pujol, M. A Langmuir Monolayer Study of the Interaction of E1 (145– 162) Hepatitis G Virus Peptide with Phospholipid Membranes. *The Journal of Physical Chemistry B*. 2009; 114(1):448–456. [PubMed: 20000622]
51. Varas M, Sánchez-Borzone M, Sánchez JM, Barioglio S. R. d. Perillo M. a. A. Surface Behavior and Peptide–Lipid Interactions of the Cyclic Neuropeptide Melanin Concentrating Hormone. *The Journal of Physical Chemistry B*. 2008; 112(24):7330–7337. [PubMed: 18503269]
52. Eeman M, Berquand A, Dufrene Y, Paquot M, Dufour S, Deleu M. Penetration of surfactin into phospholipid monolayers: nanoscale interfacial organization. *Langmuir*. 2006; 22(26):11337–11345. [PubMed: 17154623]
53. Jiang D, Dinh KL, Ruthenburg TC, Zhang Y, Su L, Land DP, Zhou F. A kinetic model for β -amyloid adsorption at the air/solution interface and its implication to the β -amyloid aggregation process. *The Journal of Physical Chemistry B*. 2009; 113(10):3160–3168. [PubMed: 19260715]
54. Sospedra P, Haro I, Alsina M, Reig F, Mestres C. Viral synthetic peptide interactions with membranes: A monolayer study. *Langmuir*. 1999; 15(16):5303–5308.
55. Ambroggio EE, Separovic F, Bowie J, Fidelio GD. Surface behaviour and peptide–lipid interactions of the antibiotic peptides, Maculatin and Citropin. *Biochimica et Biophysica Acta (BBA)-Biomembranes*. 2004; 1664(1):31–37.
56. Marczewski AW. Analysis of kinetic Langmuir model. Part I: integrated kinetic Langmuir equation (IKL): a new complete analytical solution of the Langmuir rate equation. *Langmuir*. 2010; 26(19):15229–15238. [PubMed: 20806937]
57. Peggion E, Mammi S, Schievano E. Conformation and interactions of bioactive peptides from insect venoms: The bombolitins. *Peptide Science*. 1997; 43(6):419–431. [PubMed: 9615490]
58. Fujita K, Kimura S, Imanishi Y, Rump E, Ringsdorf H. Two-dimensional assembly formation of hydrophobic helical peptides at the air/water interface: fluorescence microscopic study. *Langmuir*. 1995; 11(1):253–258.

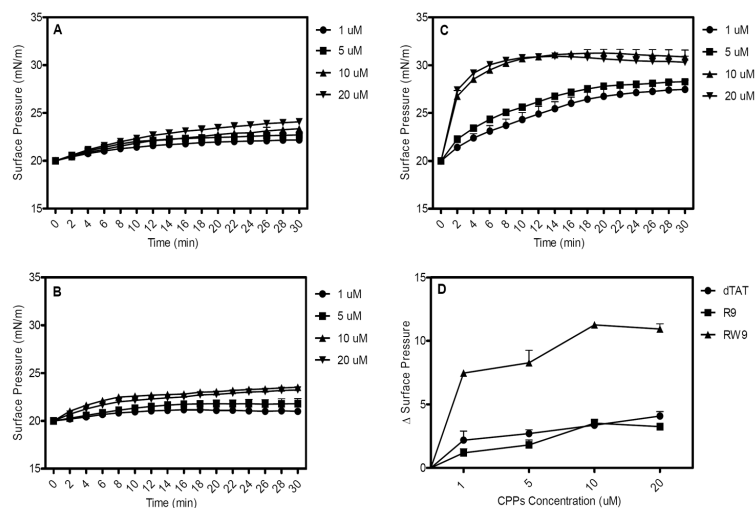


Figure 1. Changes in surface pressure recorded after adsorption of 1, 5, 10, and 20 μM of (A) dTAT, (B) R9, and (C) RW9 to a POPG phospholipid monolayer spread at an initial surface pressure of 20 mN/m. (D) The maximum change in surface pressure (plateau values) recorded at concentrations of 1, 5, 10 and 20 μM of the three CPPs. dTAT, R9, and RW9 were found to rapidly adsorb to the phospholipid monolayer. The results are presented as mean \pm SD ($n = 3$).

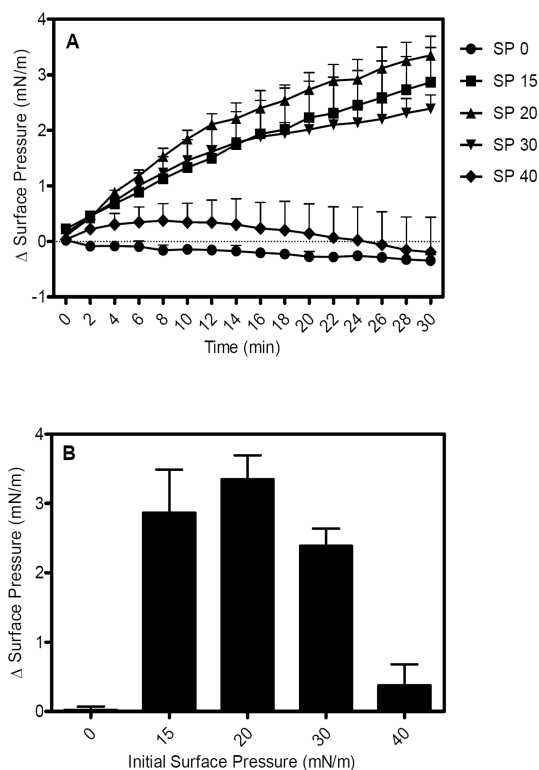


Figure 2.

(A) Time course for surface pressure changes following adsorption of dTAT peptides at a bulk concentration of $10 \mu\text{M}$ to a POPG monolayer spread at initial surface pressures of 0, 15, 20, 30 and 40 mN/m. (B) The maximum surface pressure (plateau values) reached due to peptide adsorption to the phospholipid monolayer, showing that the penetration of the CPPs is the maximum for phospholipid films held at a surface pressure of 20 mN/m. Results are presented as mean \pm SD ($n = 3$).

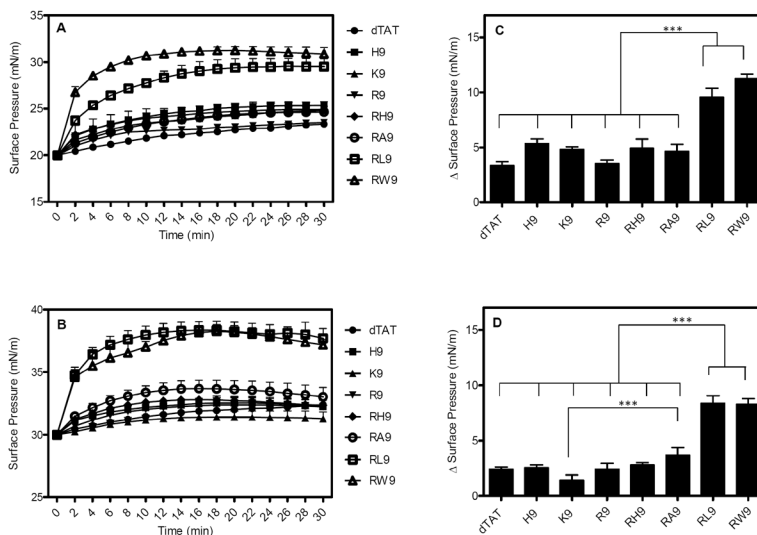


Figure 3. Changes in surface pressure as a function of time following injection of the eight CPPs below POPG monolayers held at an initial surface pressure of (A) 20 mN/m and (B) 30 mN/m. The corresponding maximum surface pressures (plateau values) recorded for the eight CPPs (peptide concentration = 10 μ M) for initial phospholipid pressures of (C) 20 mN/m and (D) 30 mN/m. The p of different peptides were compared with each CPP. Results are presented as mean \pm SD ($n = 3$), (***) = $p < 0.0001$, one-way ANOVA, Tukey post test).

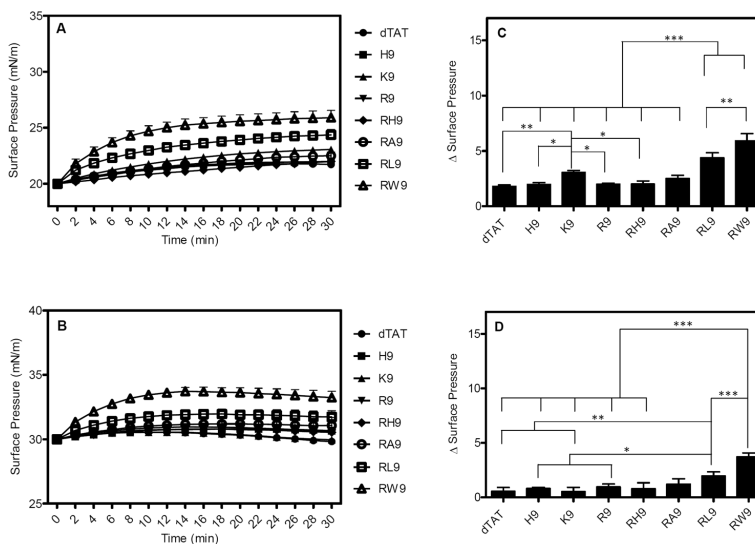


Figure 4. Changes in surface pressure as a function of time following injection of the eight CPPs below POPC monolayers held at an initial surface pressure of (A) 20 mN/m and (B) 30 mN/m. The corresponding maximum surface pressures (plateau values) recorded for the eight CPPs (peptide concentration = 10 μ M) for initial phospholipid pressures of (C) 20 mN/m and (D) 30 mN/m. The p of different peptides were compared with each CPP. Results are presented as mean \pm SD ($n = 3$), (***) = $p < 0.0001$, (**) = $p < 0.001$ and (*) = $p < 0.05$, one-way ANOVA, Tukey post test).

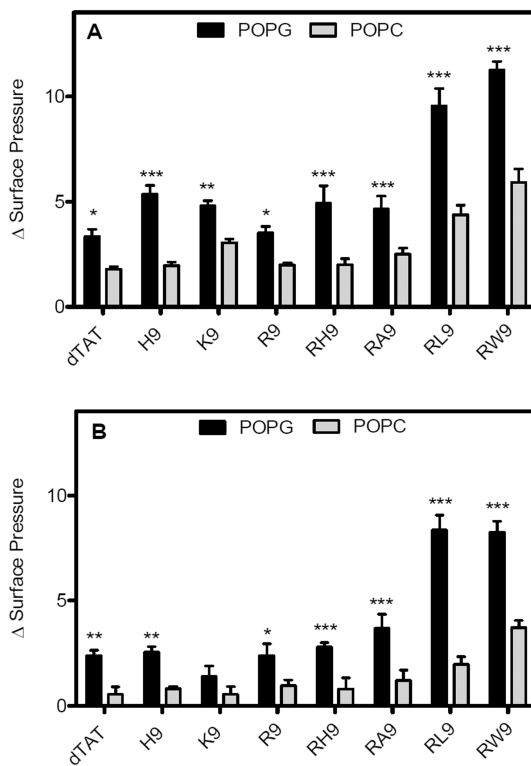


Figure 5. The maximum change in surface pressure of the phospholipid monolayers (POPG and POPC) initially held at surface pressures of 20 mN/m (A) and 30 mN/m (B) for the eight CPPs. Results are presented as mean \pm SD ($n = 3$), (***) = $p < 0.0001$, (**) = $p < 0.001$, and (*) = $p < 0.05$ unpaired t test). The p of different peptides were compared for an initial surface pressure of POPG phospholipid monolayers with POPC phospholipid monolayers for each CPPs.

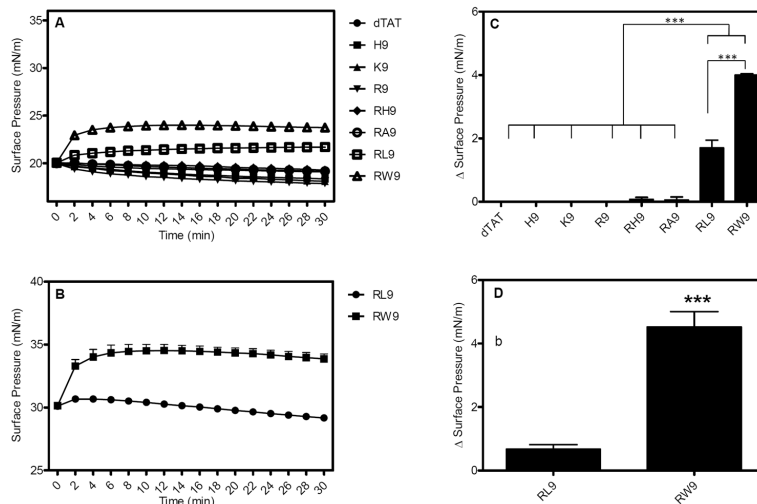


Figure 6. Surface pressure change as a function of time for a DPPC monolayer (A) at an initial surface pressure of 20 mN/m following interaction with eight CPPs (10 μ M) (B) at an initial surface pressure of 30 mN/m following injection of RL9 and RW9. The maximum change in surface pressure (plateau values) recorded for the eight CPPs at initial phospholipid surface pressure of (C) 20 mN/m for the 8 peptides and (D) 30 mN/m for RL9 and RW9. The *p* of different peptides were compared with each CPP. Results are presented as mean \pm SD (*n* = 3), (***) = *p* < 0.0001, one-way ANOVA, Tukey post test).

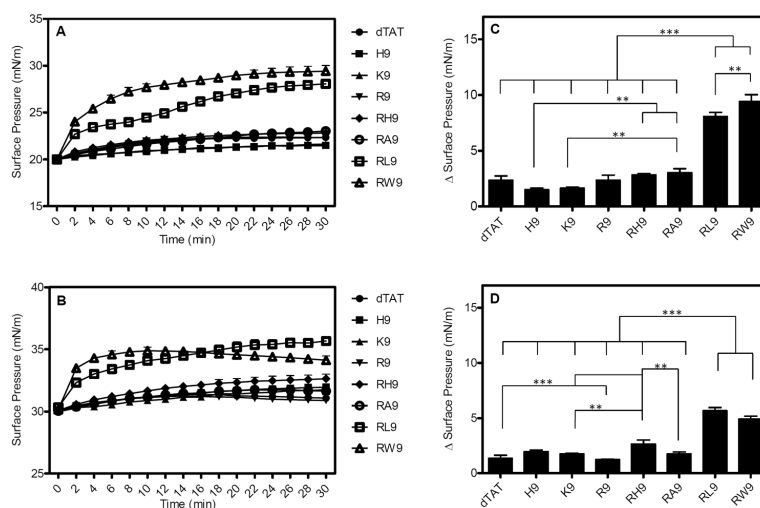


Figure 7. Changes in surface pressure as a function of time for the mixed phospholipids (POPG/DPPC) at a ratio of 1:1 held at an initial surface pressure of (A) 20 mN/m and (B) 30 mN/m, following injection of the eight CPPs into the subphase. The maximum change in surface pressure (plateau values) recorded for the phospholipids held at an initial surface pressure of (C) 20 mN/m and (D) 30 mN/m. The p of different peptides were compared with each peptide. Results are presented as mean \pm SD ($n = 3$), (***) = $p < 0.0001$, and (**) = $p < 0.001$, one-way ANOVA, Tukey post test).

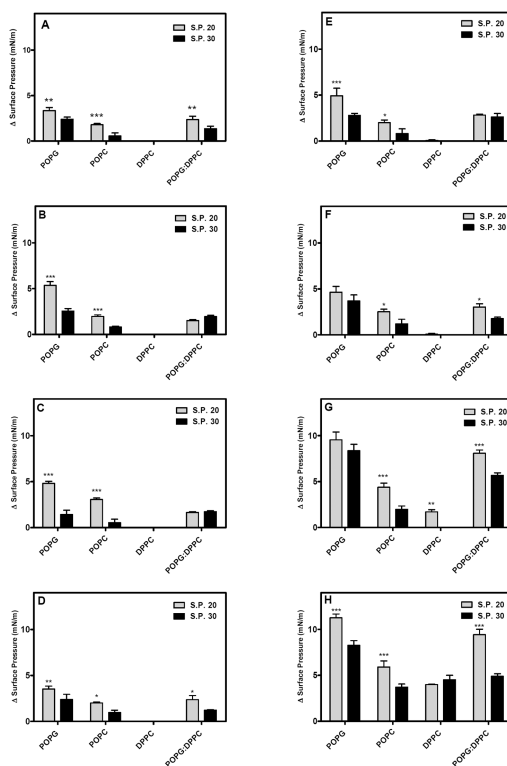


Figure 8.

Summary of results showing the maximum change in surface pressure of the phospholipid monolayers (POPG, POPC, DPPC, and POPG:DPPC) initially held at surface pressures of 20 and 30 mN/m for the eight CPPs: (A) dTAT, (B) H9, (C) K9, (D) R9, (E) RH9, (F) RA9, (G) RL9, and (H) RW9. Results are presented as mean \pm SD ($n = 3$), (***) = $p < 0.0001$, ** = $p < 0.001$, and * = $p < 0.05$ unpaired t test). The p of different peptides were compared for an initial surface pressure of 20 mN/m with 30 mN/m for each CPPs.

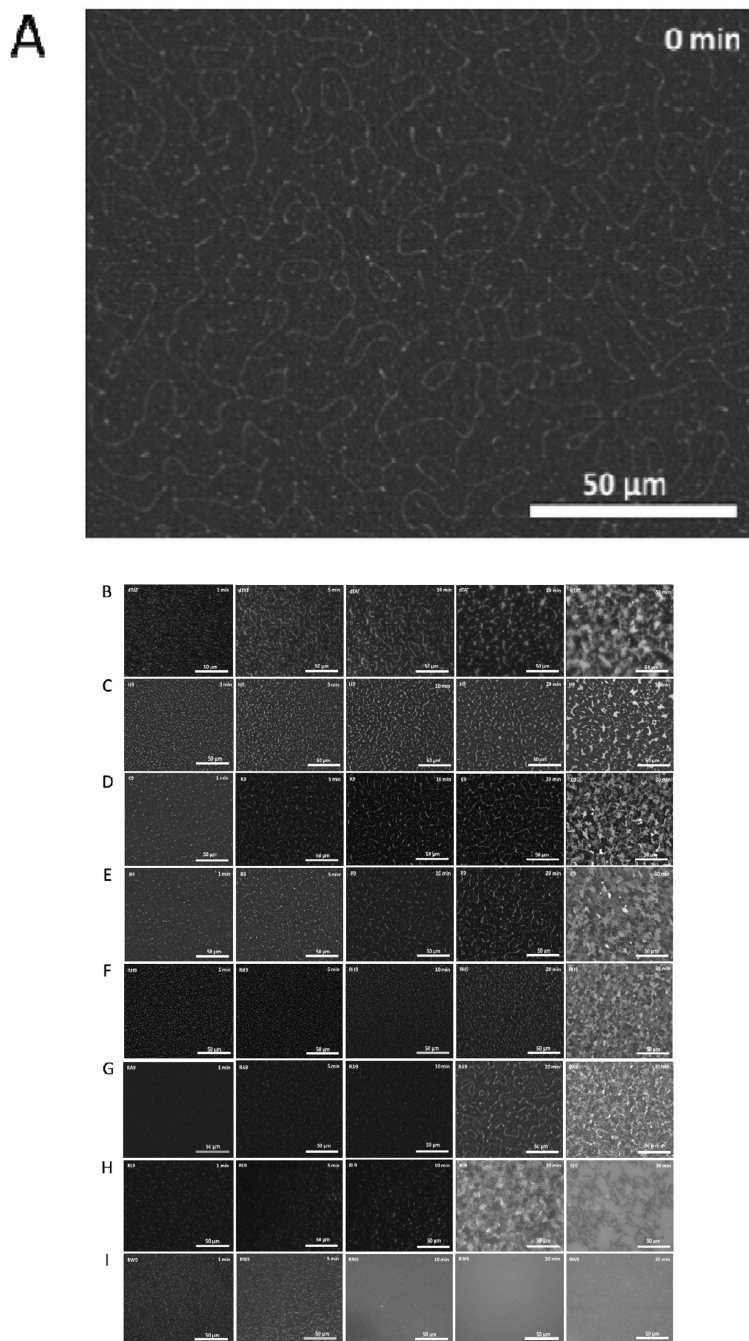


Figure 9.

Fluorescent micrographs of a POPG/DPPC (1:1) monolayer at a surface pressure of 30 mN/m on PBS buffer: (A) before injection of peptides (0 min), after injection of (B) dTAT (10 μ M) into the sub-phase, (C) H9 (10 μ M) in the sub-phase, (D) K9 (10 μ M) in the sub-phase, (E) R9 (10 μ M) in the sub-phase, (F) RH9 (10 μ M) in the sub-phase, (G) RA9 (10 μ M) in the sub-phase, (H) RL9 (10 μ M) in the sub-phase, and (I) RW9 (10 μ M) in the sub-phase. The relative increase in the bright area from 1 min to 30 min corresponds to the increase in the disordered fluid phase caused by peptides insertion. The scale bar in the lower right

represents 50 μm . The shape of the phospholipid monolayer domains change depending on the nature of the CPP.

Table 1

Name, synonyms, classification, and structure of the POPG, POPC and DPPC membrane models.

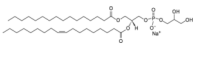
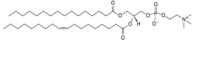
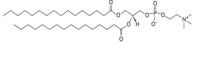
Name	Synonyms	Classification	Structure
POPG	1-hexadecanoyl-2-(9Z-octadecenoyl)-sn-glycero-3-phospho-(1'-rac-glycerol)	Anionic Phospholipid (Unsaturated)	
POPC	1-hexadecanoyl-2-(9Z-octadecenoyl)-sn-glycero-3 phosphocholine	Zwitterionic Phospholipid (Unsaturated)	
DPPC	1,2-dihexadecanoyl-sn-glycero-3-phosphocholine	Zwitterionic Phospholipid (Saturated)	

Table 2

Identification of the eight CPPs and their properties (peptide sequence, number of residues, classification, molecular weight, and sequence composition).

Name	Interpreted Sequence	Number of Residues	Classification	Molecular Weight (g/mol)	Sequence Composition (in percentage)*		
					Hydrophobic	Basic	Neutral
dTAT	R K K R R Q R R R H R R K K R	15	Hydrophilic	2200.75	0	93.33	6.67
H9	H H H H H H H H H	9	Hydrophilic	1251.38	0	100	0
K9	K K K K K K K K K	9	Hydrophilic	1170.65	0	100	0
R9	R R R R R R R R R	9	Hydrophilic	1422.74	0	100	0
RH9	R R H H R R H R R	9	Hydrophilic	1365.62	0	100	0
RA9	R R A A R R A R R	9	Amphiphilic	1167.41	33.33	66.67	0
RL9	R R L L R R L R R	9	Amphiphilic	1293.68	33.33	66.67	0
RW9	R R W W R R W R R	9	Amphiphilic	1512.83	33.33	66.67	0

* Hydrophobic/ Neutral/ Basic amino acid % = $(N_x/N) \times 100$, N_x : Number of hydrophobic/ neutral/ basic amino acid residues present in the input sequence. N: Input sequence length (net charge at neutral pH).